

High Temperature Creep Behaviour of β' - $\text{Si}_3\text{N}_4/\alpha$ -YSiAlON Ceramics

G. Bernard-Granger,^{a*} J. Crampon,^b R. Duclos^{b†} & B. Cales^c

^aSaint Gobain/Norton Research Center, Goddard Road, Northboro, MA 01532-1545, USA

^bLaboratoire de Structure et Propriétés de l'Etat Solide, URA CNRS 234, Bat C6, Université des Sciences et Technologies de Lille, 59655 Villeneuve d'Ascq Cedex, France

^cNORTON Desmarquest Fine Ceramics, Research Center, Z.I. n° 1, 27025 Evreux Cedex, France

(Received 18 October 1996; revised version received 28 November 1996; accepted 2 December 1996)

Abstract

The improvement in high temperature mechanical properties of silicon nitride ceramics has been explored by fabrication of a β' - $\text{Si}_3\text{N}_4/\alpha$ -YSiAlON ceramic densified, without additives and without HIP treatment, by sintering of a mixture of α - Si_3N_4 and α -YSiAlON powders under a nitrogen pressure of 5 MPa. The high temperature creep behaviour was investigated in the ranges 100–400 MPa and 1280–1400°C by compressive tests. The creep performances were very impressive. The activation energy ($Q = 770$ kJ/mol) and the stress exponent ($n = 1$) are consistent with a deformation mechanism resulting from grain boundary sliding accommodated by volume diffusion. Microstructure was not affected by the deformation conditions, in particular no cavity formation was observed after creep at 1400°C and 300 MPa. This behaviour is related to the probable absence of a thick boundary film which may result from crystallization during cooling of small glass pockets and from internal stresses caused by the volume change of crystallizing pockets. © 1997 Elsevier Science Limited.

L'amélioration des propriétés mécaniques de haute température de nitrures de silicium a été explorée par fabrication d'une nuance β' - $\text{Si}_3\text{N}_4/\alpha$ -YSiAlON, obtenue à partir d'un mélange de poudres commerciales de α - Si_3N_4 et α -YSiAlON, densifiée sans ajouts par frittage dans une atmosphère de 5 MPa d'azote. Le comportement en fluage a été étudié entre 1280 et 1400°C au cours d'essais en compression dans la gamme 100–400 MPa. La résistance au fluage est très remarquable pour ces conditions d'essais. L'énergie d'activation ($Q = 770$ kJ/mole)

et l'exposant de contrainte ($n = 1$) sont en accord avec du glissement aux joints accommodé par la diffusion en volume. La microstructure n'a pas été affectée par la déformation, en particulier aucune cavitation n'a été notée pour les conditions d'essais extrêmes. Ceci peut être corrélé à l'absence probable d'un film intergranulaire amorphe d'épaisseur nanométrique. La cristallisation de poches vitreuses au cours du refroidissement et les contraintes qui en résultent en seraient alors à l'origine.

1 Introduction

Because of their highly covalent Si–N bonds and low diffusion coefficients,¹ sintered silicon nitrides (SSN) are usually densified with the aid of additives which form a liquid phase at the sintering temperature promoting matter transport by the liquid phase sintering mechanism.² Unfortunately, on cooling, the liquid generally transforms into a residual intergranular amorphous phase whose quantity, distribution and chemical composition control the mechanical properties^{3–7} at high temperature. In order to minimize the amount of vitreous phase, several techniques have been tested such as crystallization heat treatments which improve the creep resistance by limiting the viscous flow in the recrystallized phases.^{8,9} Nevertheless, when heat treating SSN, the thin vitreous film, which generally subsists between the new crystalline phases and the nitride grains,^{10,11} continues to control the high temperature behaviour.⁷ The best properties are obtained by using a high pressure densification technique (HIP) with only the native SiO_2 coating on Si_3N_4 grains or with a low level of yttria, for instance.^{12,13} The main disadvantage of that technique lies in the necessity of encapsulating the green compact, a somewhat complicated and expensive process.

*Now at NORTON Desmarquest Fine Ceramics, 27025 Evreux, France.

†To whom correspondence should be addressed.

Another way to reduce the quantity of vitreous phase may consist in using sintering additives able to be dissolved into the Si_3N_4 crystal structure and to form SiAlON ceramics.

The last solution has been experimentally investigated¹⁴⁻¹⁷ and has indeed shown a marked increase in creep resistance as the composition of maximum substitution is approached. This was correlated to a decrease in the grain boundary phase amount. Since these earlier works, numerous studies related to the achievement of sialon ceramics with various oxide additives leading to β or mixed α - β sialons have been undertaken (see Ref. 18, for instance). However, the preparation technique of these sialon materials is not always well adapted to the requirements of an industrial fabrication process particularly when volatile mixing media or hot isostatic pressing are used, the latter not being adapted for mass production of ceramics of complicated shapes.

In this paper an alternative route which allows us to obtain a β' - $\text{Si}_3\text{N}_4/\alpha$ -YSiAlON ceramic densified without sintering additives and without HIP treatment is presented. This silicon nitride ceramic exhibits very large creep resistance up to 1400°C; this will be discussed relative to the very reduced glassy phase content.

2 Experimental procedure

The starting materials were α - Si_3N_4 (SN-E-10, UBE) and α -YSiAlON (SY5, UBE, manufacturer composition: $\text{Y}_{0.5}\text{Si}_{9.75}\text{Al}_{2.25}\text{O}_{0.75}\text{N}_{15.25}$) powders. Their main physical and chemical characteristics are given in Table 1. They were mixed in water in the volume ratio 60:40 and milled in polyethylene jars with Si_3N_4 balls. After spray drying, discs were cold pressed, embedded in Si_3N_4 powder (SN-E-10) and then sintered at 1800°C under a nitrogen pressure of 5 MPa (gas pressure sintering, GPS) maintained to 1200°C during cooling. The microstructure of sintered materials was studied by transmission electron microscopy (TEM) at 300 kV (Philips CM30, theoretical resolution: 0.21 nm) at two scales: (i) at the micrometer scale

Table 1. Main physical and chemical characteristics of as-received powders

	<i>Ube SNE10</i>	<i>Ube SY5</i>
Particle size (μm)	0.2	0.5-2
Surface area (m^2/g)	10	1-2
Crystallinity	$\alpha > 95\%$	100% α
Purity	N > 38% O < 2% C < 0.2%	metal < 200 p.p.m.
	Cl, Fe < 100 p.p.m. Ca, Al < 50 p.p.m.	

to evaluate the shape, distribution and composition (determined by energy dispersive X-ray spectroscopy (EDS)) of the different phases and (ii) at the nanometer scale by high resolution TEM (HRTEM) to characterize the various kinds of interface. These techniques were also used to characterize the structure changes after deformation.

At room temperature the Vickers hardness and toughness, determined on five specimens by the indentation crack size measurement technique¹⁹ under a load of 10 kg, were 15.5 ± 0.3 GPa and 6.1 ± 0.2 MPa $\text{m}^{1/2}$, respectively. A flexural strength of 905 ± 20 MPa was measured by three point bending tests.

The high temperature mechanical behaviour was determined by compressive creep tests in air between 1280 and 1400°C in a relatively large stress range (100-400 MPa). The creep samples were 3 mm \times 3 mm \times 7 mm. The steady state creep rate $\dot{\epsilon}$ was related to the applied stress σ and to the temperature T by the classical Norton law:

$$\dot{\epsilon} = A(s) \sigma^n \exp(-Q/RT) \quad (1)$$

where $A(s)$ is a constant depending on the material structure, n is the stress exponent, Q is the creep activation energy and R is the universal gas constant. In order to minimize the influence of microstructure dispersion on the determination of parameters n and Q , these were measured by the stress or temperature change technique,²⁰ i.e. by modifying the applied stress or the temperature during a test at constant temperature or stress, respectively, and by comparing the strain rates before and after the change. The activation energy and stress exponent were determined within 50 kJ/mol and 0.1, respectively.

3 Results

3.1 Microstructural characterization of as-sintered materials

Figure 1 presents the typical microstructure of the material. It is mainly composed of two kinds of grain: β' - Si_3N_4 and α -YSiAlON grains. The β' phase consisted of needles or of regular shaped polygons according to the orientation of the grains relative to the cross-sectional plane. Concerning the α grains, their shape looked like that of amorphous phase pockets in sintered silicon nitrides.²¹ This morphology is different from that reported by Olsson and Ekström²² for mixed α - β sialons densified with Y_2O_3 and La_2O_3 additives, α grains being elongated in their case. EDS microanalyses showed that the two kinds of grain were substituted in Al and O, a little more for the

α grains which also contained yttrium, explaining the darker aspect of these grains. More precisely, the composition of β' grains and α grains was $\text{Si}_{10.99}\text{Al}_{1.01}\text{O}_{1.01}\text{N}_{14.99}$ and $\text{Y}_{0.3}\text{Si}_{10.44}\text{Al}_{1.56}\text{O}_{0.66}\text{N}_{15.34}$, respectively. Using the Yeheskel method²³ the β' - Si_3N_4 and α -YSiAlON grains were found to be in the approximate ratio 75:25.

In addition, the following two minor phases were also observed: (i) An yttrium-rich crystalline phase (Fig. 2) segregated in the shape of small isolated pockets located at the triple points of the β' grains. The composition of these pockets was not constant throughout the specimens; a majority of these grains had a composition near $\text{Si Al}_{0.26}\text{Y}_{1.07}\text{O}_4$ or $\text{Si Al}_{0.48}\text{Y}_{2.19}\text{O}_6$ (EDS analyses do not allow us to conclude that nitrogen is present in these phases) but their structure was not determined. (ii) Very small glassy pockets located near the α -YSiAlON grains (Fig. 3). On the other hand no amorphous film was detected by HRTEM at the α/β' and α or β'/Y -rich crystalline phase interfaces (Figs 4-6). From these observations it is not possible to claim with assurance that no intergranular film at all was present in our materials. They only suggest that the film, if present, was so thin that it was difficult to observe it with the present resolution.

Similar observations have already been reported by Ukyo and Wada^{24,25} in the case of fine-grained ($\alpha + \beta$) SiAlON ceramic composites obtained by hot pressing mixtures of Si_3N_4 , Al_2O_3 and AlN. These authors showed that for some hot pressing conditions, grain boundaries and triple points could be free of a glass phase and when present, according to hot pressing temperature, the glass phase was found in very small quantities at multiple-grain junctions.

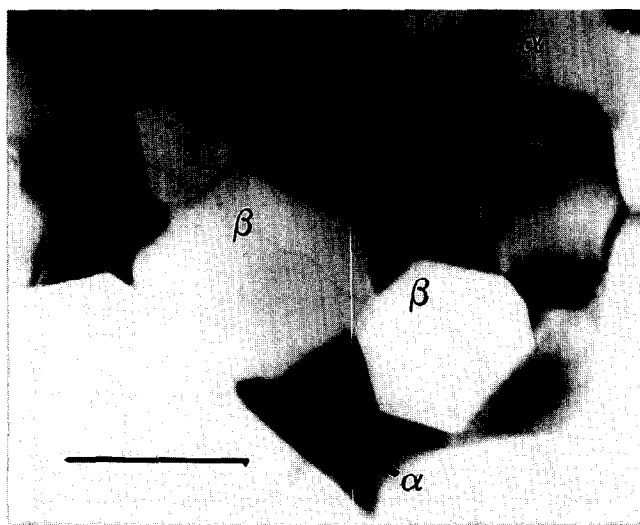


Fig. 1. Typical microstructure of β' - $\text{Si}_3\text{N}_4/\alpha$ -YSiAlON material in as-sintered condition showing two kinds of grain. The α grains are the dark ones. Bar = 0.3 μm .

3.2 Creep behaviour

Figure 7 shows some creep curves obtained under a stress of 300 MPa in the temperature domain

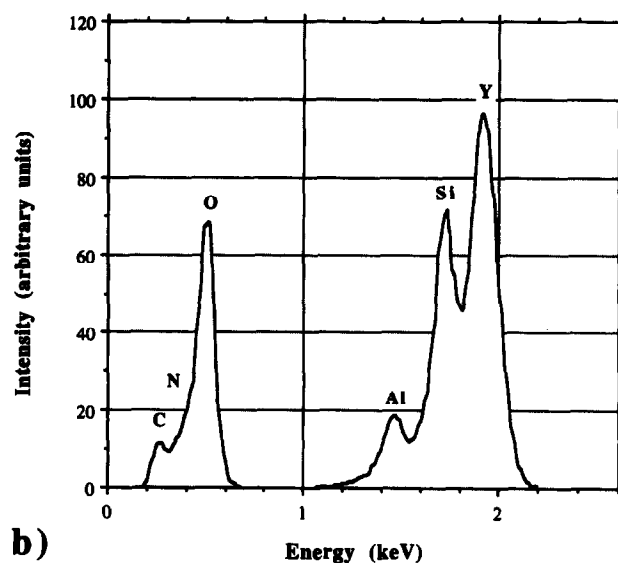


Fig. 2. (a) Crystallized pockets located at the triple points of the β' phase. Bar = 0.5 μm . (b) EDS analysis of the pockets. The presence of nitrogen is difficult to assess.



Fig. 3 Small glass pocket located at a triple point between grains of the two phases. Bar = 0.5 μm .

1280–1400°C. The steady state creep was reached after a transient creep of a few tens of hours. Even at 1400°C the ultimate strain obtained after more than 120 h is small (less than 1%) and the corresponding creep rate very low (less than 10^{-9} s^{-1} at 1280°C and about $2 \times 10^{-7} \text{ s}^{-1}$ at 1400°C). No creep acceleration was observed for the following experimental conditions: 1280–1400°C; 100–400 MPa; test duration <150 h. In these domains the stress exponent n and the activation energy Q were constant and equal to 1 and 770 kJ/mol, respectively.

3.3 TEM of crept samples

Observations were made in samples crept at 1280, 1320 and 1400°C. It appeared that no noticeable structure change associated with deformation could be detected in the crept samples (Fig. 8). No cavity nucleation and no extensive dislocation activity were observed after creep, even at 1400°C under a

stress of 400 MPa. The only modification that was noted concerns the α -YSiAlON grains which seemed to be slightly larger than in as-sintered specimens.

4 Discussion

4.1 Microstructure of as-sintered specimens

The structure of the as-sintered material and especially the morphology of α -YSiAlON grains as the small crystallized pockets containing all the species are consistent with a liquid phase sintering process. At the sintering temperature, Y^{3+} and Al^{3+} cations diffused from α -YSiAlON grains and reacted with the thin silica coating present on the α - Si_3N_4 grains to form a liquid phase which promoted the α - $\text{Si}_3\text{N}_4 \rightarrow \beta$ '- Si_3N_4 conversion and also the partial change, by a dissolution/transport/precipitation mechanism, of α -YSiAlON into

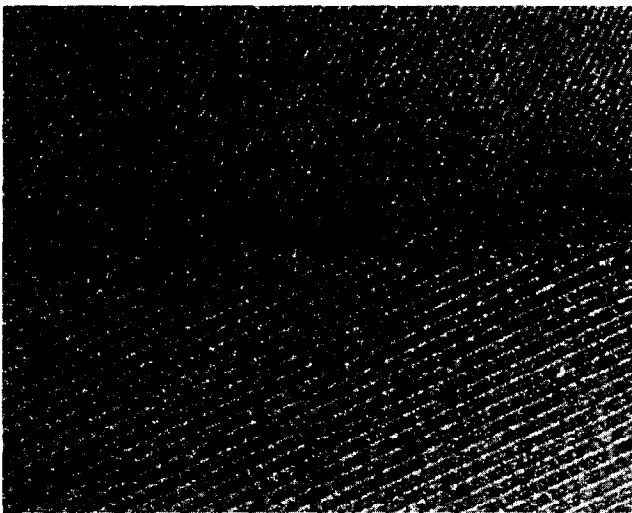


Fig. 4. HTREM of a α {(top), (2110) planes}/ β ' {(bottom), (1010)} interface. Bar 5 nm.

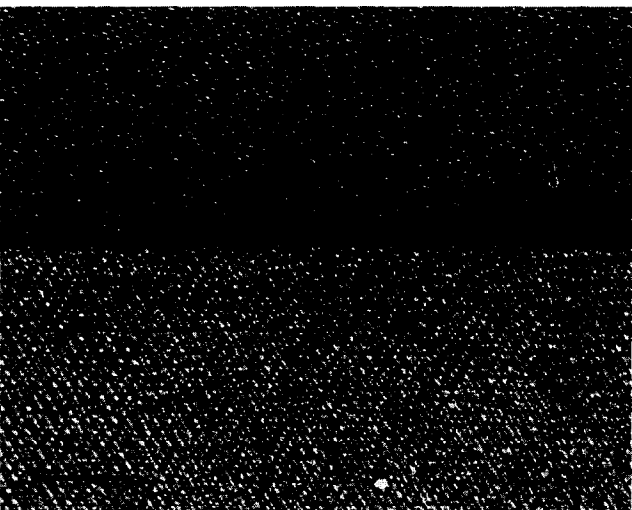


Fig. 5. HTREM of a β/β ' interface; (1010) planes imaged in the bottom part. Bar = 5 nm.

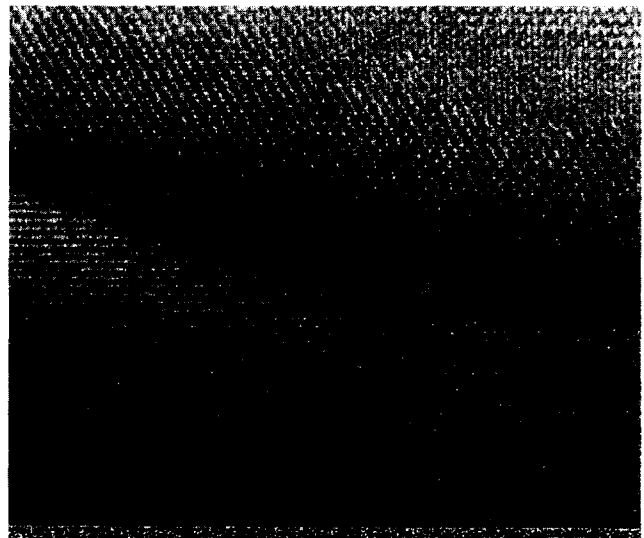


Fig. 6. HTREM of a phase recrystallized (bottom)/ β ' {(top), [0001] vertical} interface. Bar = 5 nm.

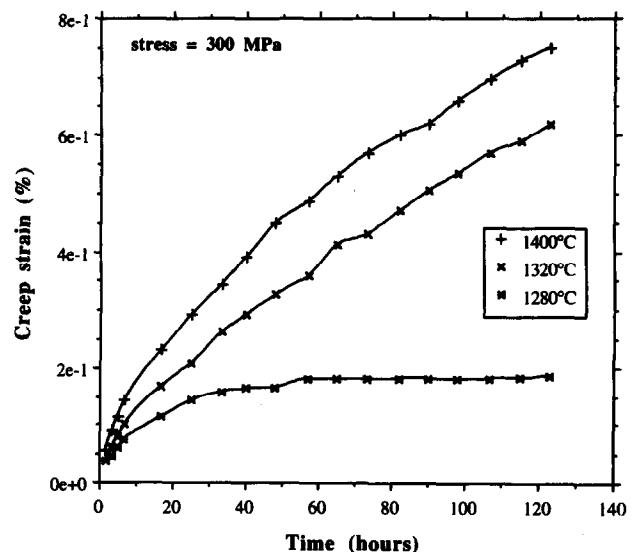


Fig. 7. Influence of temperature on creep strain versus time curves at 300 MPa.

β' - Si_3N_4 in consideration of the final ratio between these two phases. But as this latter transformation was probably not complete at the sintering temperature, a large amount of the liquid phase in contact with the remaining α -YSiAlON grains devitrified during cooling and precipitated on these grains. On the other hand, probably due to a propitious composition, the liquid in between the β' grains crystallized to form an yttrium-rich phase, owing to the very low solubility of yttrium in surrounded grains. Last, due to energy criteria,²⁶ devitrification could not be complete and some rare small amorphous pockets subsisted at triple points near α -grains. The nature of the various interfaces (is a glass boundary film present or not?) will be discussed latter.

4.2 Creep mechanisms

The main characteristic of this material is its impressive creep resistance up to 1400°C. In Fig. 9 we compare for the same experimental conditions



Fig. 8. Microstructure after deformation at 1400°C and 300 MPa over 120 h. Bar = 0.5 μm .

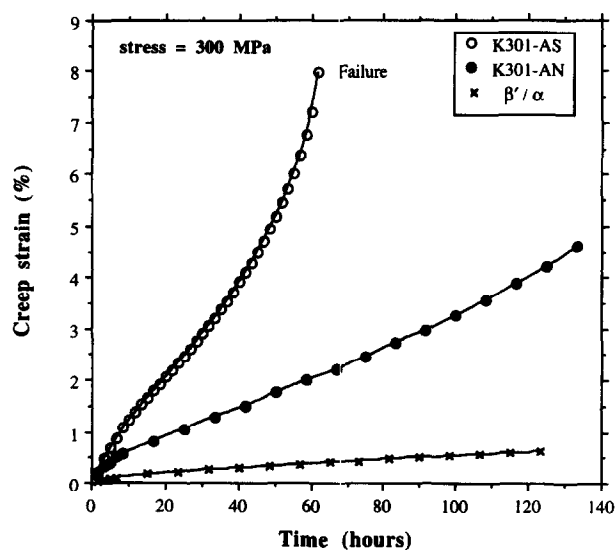


Fig. 9. Comparison at 1320°C and 300 MPa of creep curves of as-sintered (AS) and annealed (AN) Kersit 301 and β' - $\text{Si}_3\text{N}_4/\alpha$ -YSiAlON specimens.

(1320°C, 300 MPa) the creep curve of this material to those of two samples of a commercial SSN (Kersit 301, C.T. Desmarquest, Evreux, France) densified with 10 wt% of a mixture of Y_2O_3 , Al_2O_3 and AlN :²⁷ an as-sintered specimen and an annealed one of which about 98% of the original amorphous phase was crystallized,²¹ with a thin glass boundary film subsisting at the various interfaces. The difference in creep behaviour is spectacular. The creep rates of the β'/α material are about comparable with those reported by Ferber *et al.* for a Norton NT 164 ceramic,²⁸ a silicon nitride HIPed with 4% yttria.

For the Kersit 301 material, the passage from diffusional to cavitation creep appeared in particular by a change in the stress exponent n ($n = 1$ and $n = 2$, respectively).⁷ Presently, for the β' - $\text{Si}_3\text{N}_4/\alpha$ -YSiAlON material, the steady state creep rate was related to stress and temperature in the whole experimental domain by only one relationship in which the stress exponent was 1 and the activation energy 770 kJ/mol. The absence of cavity formation and of an obvious plasticity resulting from intragranular dislocation glide, as the thermomechanical parameters, are consistent with a deformation mechanism controlled by matter diffusion and grain boundary sliding. In silicon nitride matter, transport is generally related to a solution/diffusion/reprecipitation mechanism through the amorphous intergranular phase. In the present case the presence of such a phase is not evident:

- (1) HRTEM did not allow us to observe that phase. One can think that its thickness is very small, of the same order as the film thickness reported by Ferber *et al.*²⁸ for the Norton NT164 material ($\ll 1$ nm). In that case one can ask about the meaning of an intergranular film whose thickness is about the size of a silica tetrahedron (is it really a vitreous film?) and about its influence on matter diffusion.
- (2) The absence of cavitation at triple points could arise because either diffusion is fast enough to release the stress concentration owing to grain boundary sliding, or grain boundary sliding is rendered difficult owing to the absence of a low viscosity intergranular film. This latter point seems to be more accurate at present. The critical stress needed to nucleate boundary cavities is then increased with respect to a material containing a vitreous phase.²⁹ The same conclusion was given by Ferber *et al.*²⁸ when these authors compared the cavitation behaviour of NT 154 and NT 164 materials.

- (3) When cooled under load, specimens containing a vitreous film generally show on TEM micrographs some strain whorls typical of viscoelastic effects induced by the glass phase.^{30,31} Such contrasts were never observed in this material.

Concerning the activation energy (770 kJ/mol), the range of reported values is large enough to account for this value and the comparison is therefore not determinant. So as only small glassy pockets segregated at triple points were observed, we assume that for this material a pure diffusional mechanism could be the controlling mechanism. The activation energy value, 770 kJ/mol, is close to the value of 780 kJ/mol determined by Kijima and Shirasaki³² for the bulk diffusion of nitrogen in Si₃N₄. Using the classical Nabarro–Herring model:³³

$$\dot{\epsilon} = 14 \sigma \Omega D_V / RTd^2 \quad (2)$$

where Ω is the diffusing species volume, D_V the volume diffusion coefficient value and d the grain size, $\dot{\epsilon}$, σ , R and T having the same meaning as in relation (1), we found a value of the volume diffusion coefficient of 7.2×10^{-22} m²/s at 1360°C compared to 1.6×10^{-22} m²/s in the literature¹ and 3.6×10^{-23} m²/s compared to 2.5×10^{-23} m²/s at 1280°C. The relevant parameters for calculation were: $\sigma = 300$ MPa, $\Omega = 7 \times 10^{-29}$ m³ and creep rates equal to 1.9×10^{-8} s⁻¹ and 10^{-9} s⁻¹ at 1360 and 1280°C, respectively. The agreement with the literature data is good enough to support the hypothesis of a grain boundary sliding mechanism accommodated by volume diffusion.

4.3 Discussion on the nature of interfaces

As already presented, the presence of an intergranular film was questionable in this material. As a comparison, Fig. 10 shows a film observed with

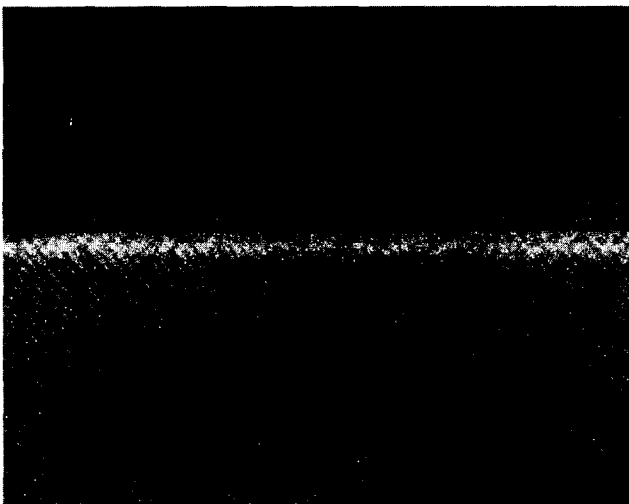


Fig. 10. HTREM of a β/β interface in a silicon nitride sintered with 1 wt% of additives. Bar = 5 nm.

the same resolution in a silicon nitride HIPed with 1 wt% of Y₂O₃ and Al₂O₃ additives.^{31,34} Such an observation was not made in the present material. What would be the reason why such a film was not observed? According to the Clarke model¹⁰ the stability of a thin glassy film is dependent upon the balance between attractive Van der Waals forces and repulsive steric forces acting on the film. The net force per unit area of film is:

$$F_{\text{net}}(\text{Pa}) = (H_{\text{NgN}}/6\pi h^3) - 4 a \eta_0^2 \exp(-h/\xi) \quad (3)$$

where H_{NgN} is the Hamaker constant of a nitride/glass/nitride interface, h is the film thickness, $a\eta_0^2$ is the free energy density difference between an ordered and a disordered film and ξ is a structural correlation length. The Hamaker constant has been calculated by using the Israelachvili expression and the values of the refractive indices and dielectric constants of the interface materials given in Ref. 10. It can be written versus temperature as:

$$H_{\text{NgN}}(\text{J}) = 1.3 \times 10^{-24} T + 7.61 \times 10^{-20} \quad (4)$$

By taking a correlation length ξ equal to the size of a SiO₄ tetrahedron (0.3 nm) and a value of 400 MPa for the constant a ,¹⁰ the expression for the net force at 1800°C is:

$$F_{\text{net}}(\text{Pa}) = (4.18 \times 10^{-21}/h^3) - 16 \times 10^8 \eta_0^2 \exp(-h/3 \times 10^{-10}) \quad (5)$$

In Fig. 11 the variation of the net force per unit area is presented at the sintering temperature for values of the parameter η_0 equal to 0.3 and 0.5. Due to the lack of reliable values for the various constants, the above calculation is only approximate. Moreover, as shown by Clarke,¹⁰ the pressure required to remove the intergranular film is strongly dependent on the value of η_0 .

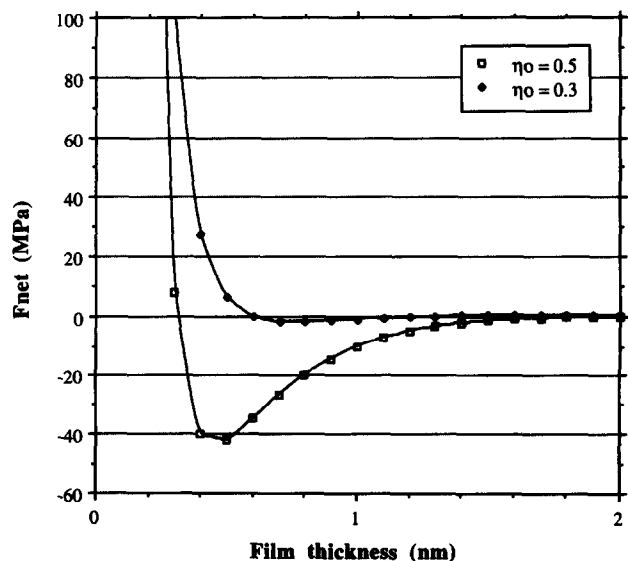


Fig. 11. Variation of net force as a function of boundary film thickness at 1800°C for two values of h_0 : 0.3 and 0.5.

For $\eta_0 = 0.5$, a compressive stress of 40 MPa would be necessary. The values of η_0 in Fig. 11 assume that the orientation relations between SiO_4 tetrahedra and neighbour grains are far from the complete epitaxy. In particular, these values can increase when the thickness of the film becomes smaller and smaller and consequently the SiO_4 entities get nearer and nearer. However, we do not think that the film thickness reduction arose at the sintering temperature because crystallization of glass pockets, without possible matter flow into these pockets, would not have been complete due to energy criteria.²⁶ Consequently this would have entailed a glass film between crystallized pockets and surrounding grains. This film is not observed. Nevertheless after sintering some glass was found in the Si_3N_4 powder bed close to the surface of the discs. This observation supports the possibility that an amount of the vitreous phase was able to diffuse from the bulk into the external powder bed during sintering.

On the other hand, we think that the nitrogen pressure and a propitious composition of the glassy phase have been able to favour the crystallization onset of the pockets at a temperature where the glassy phase viscosity was low. The volume change connected with crystallization of those pockets could then be compensated by matter flows from boundaries generated by non-hydrostatic compressive stresses created by this volume change. Indeed, volume changes due to crystallization lead to internal stresses. Their consequences on crystallization have been studied by Kessler *et al.*³⁵ who concluded that these stresses could be relaxed either by a flow of glassy phase from two grain-junctions into crystallizing pockets or by dissolution of primary grains in the intergranular film, transport and reprecipitation at the boundary of pockets. These stress relaxation mechanisms correspond to a constant grain size or to a constant film thickness, respectively. However theoretical considerations only are not adequate to decide on the rate controlling mechanism. Moreover, the goal of our experiments was not to determine the crystallization kinetics during cooling (the furnace used for the experiments was not adapted to fast cooling), and the chemistry of the film between the sintering temperature and the crystallization onset, which is a very important parameter for this process, is not known.

In the present case it is thus assumed that the stresses induced by the volume change due to crystallization were relaxed by a matter flow from two grain-junctions into crystallizing pockets. The quantity of intergranular amorphous phase is thus reduced up to an 'equilibrium' thickness depending on these stresses.

5 Conclusions

In this paper the fabrication process of an α/β SiAlON has been presented. A mixture of α - Si_3N_4 and α - YSiAlON powders was densified by GPS at 1800°C in a nitrogen atmosphere of 5 MPa. This low cost method is very convenient for the production of ceramics of complicated shapes. The high temperature mechanical properties have been characterized by compressive creep tests performed up to 1400°C. The creep rates were comparable to those of a HIPed Norton NT 164 ceramic.²⁸ This very strong creep resistance seems to be connected with the absence of an intergranular film at the different interfaces. We think that owing to crystallization of the glass pockets at a high temperature, when the glass phase viscosity was low, the compressive internal stresses connected with the volume change of crystallizing pockets were large enough to squeeze out the main part of the film from boundaries into pockets to release these stresses.

References

1. Ziegler, G., Heinrich, J. and Wotting, G., Relationships between processing, microstructure and properties of dense and reaction-bonded silicon nitride. *J. Mater. Sci.*, 1987, **22**, 3041–3086.
2. Kingery, W. D., Densification during sintering in the presence of a liquid phase. I. Theory. *J. Appl. Phys.*, 1959, **30**, 301–306.
3. Kleebe, H.-J., Cinibulk, M. K., Cannon, R. M. and Ruhle, M., Statistical analysis of the intergranular film thickness in silicon nitride ceramics. *J. Am. Ceram. Soc.*, 1993, **76**, 1969–1977.
4. Cinibulk, M. K., Kleebe, H.-J., Schneider, G. A., and Ruhle, M., Amorphous intergranular films in silicon nitride ceramics quenched from high temperatures. *J. Am. Ceram. Soc.*, 1993, **76**, 2801–2808.
5. Tanaka, I., Igashira, K., Kleebe, H.-J. and Ruhle, M., High temperature strength of fluorine-doped silicon nitride. *J. Am. Ceram. Soc.*, 1994, **77**, 275–277.
6. Tanaka, I., Kleebe, H.-J., Cinibulk, M. K., Burley, J., Clarke, D. R. and Ruhle, M., Calcium concentration dependence of the intergranular film thickness in silicon nitride. *J. Am. Ceram. Soc.*, 1994, **77**, 911–914.
7. Bernard-Granger, G., Devitrification of the intergranular phase in silicon nitrides. Influence on the high temperature mechanical properties. Ph.D. thesis, University of Lille 1, Villeneuve d'Ascq, France, 1994.
8. Cinibulk, M. K., Thomas, G. and Johnson, S. M., Grain-boundary-phase crystallization and strength of silicon nitride sintered with a YSiAlON glass. *J. Am. Ceram. Soc.*, 1990, **73**, 1606–1612.
9. Chen, C. F. and Tien, T. Y., Microstructural effect on creep of silicon nitride ceramics. *Mater. Sci. For.*, 1989, **47**, 204–214.
10. Clarke, D. R., On the equilibrium thickness of intergranular glass phases in ceramics materials. *J. Am. Ceram. Soc.*, 1987, **70**, 15–22.
11. Thorel, A., Atomic structure of interfaces in SiAlON silicon nitride ceramics. Ph.D. thesis, Ecole des Mines de Paris, Paris, France, 1988.

12. Homma, K., Okada, H., Fukijawa, T. and Tatuno, T., HIP Sintering of silicon nitride without additives. *Yogyo-Kyokai-Shi*, 1987, **95**, 29–34.
13. Klemm, H. and Pezzotti, G., Fracture toughness and time-dependent strength behavior of low-doped silicon nitride for applications at 1400°C. *J. Am. Ceram. Soc.*, 1994, **77**, 553–561.
14. Jack, K. H., Sialons and related nitrogen ceramics. *J. Mater. Sci.*, 1976, **11**, 1135–1158.
15. Lumby, R. J., North, B. and Taylor, A. J., In *Special Ceramics 6*, ed. P. Popper. British Ceramic Research Association, Stoke on Trent, UK, 1974, pp. 283–298.
16. Lewis, M. H., Powell, B. D., Drew, P., Lumby, R. J., North, B. and Taylor, A. J., The formation of single-phase Si–Al–O–N ceramics. *J. Mater. Sci.*, 1977, **12**, 61–74.
17. Mitomo, M., Kuramoto, N. and Inomata, Y., Fabrication of high strength β -Sialon by reaction sintering. *J. Mater. Sci.*, 1979, **14**, 2309–2316.
18. Ekström, T. and Nygren, M., SiAlON ceramics. *J. Am. Ceram. Soc.*, 1992, **75**, 259–276.
19. Niihara, K., Morena, R. and Hasselman, D. P. H., Indentation fracture toughness of brittle materials for Palmqvist cracks. In *Fracture Mechanics of Ceramics*, Vol. 5, ed. R. C. Bradt, A. G. Evans, P. P. Hasselman and F. F. Lange. Plenum Press, New York, 1983, pp. 97–105.
20. Poirier, J.-P., *Plasticité à Haute Température des Solides Cristallins*. Eyrolles, Paris, 1976, pp. 37–42, 55–56.
21. Bernard-Granger, G., Crampon, J., Duclos, R. and Cales, B., Glassy grain-boundary phase recrystallization of silicon nitride: kinetics and phase development. *J. Mater. Sci. Lett.*, 1995, **14**, 1362–1365.
22. Olsson, P.-O. and Ekström, T., HIP-sintered β and mixed α - β sialons densified with Y_2O_3 and La_2O_3 additions. *J. Mater. Sci.*, 1990, **25**, 1824–1832.
23. Yeheskel, O., Gefen, Y. and Talianker, M., Hot isostatic pressing of Si_3N_4 with Y_2O_3 additions. *J. Mater. Sci.*, 1984, **19**, 745–752.
24. Ukyo, Y. and Wada, S., High strength Si_3N_4 ceramics. *Nippon Seramikkuso Kyokai Gakujutsu Ronbunshi*, 1989, **97**, 872–874.
25. Wada, S. and Ukyo, Y., Microstructures and properties of α/β SiAlON composite. Paper presented at the Japan Congress on Material Research, 1990.
26. Raj, R. and Lange, F. F., Crystallization of small quantity of glass (or a liquid) segregated in grain boundaries. *Acta Metall.*, 1981, **29**, 1993–2000.
27. Lakki, A., Schaller, R., Bernard-Granger, G. and Duclos, R., High temperature anelastic behaviour of silicon nitride studied by mechanical spectroscopy. *Acta Metall. Mater.*, 1995, **43**, 419–426.
28. Ferber, M. K., Jenkins, M. G., Nolan, T. A. and Yeckley, R. L., Comparison of the creep and creep rupture performance of two HIPed silicon nitride ceramics. *J. Am. Ceram. Soc.*, 1994, **77**, 657–665.
29. Evans, A. G., Rice, J. R. and Firth, J. P., Suppression of cavity formation in ceramics: prospects for superplasticity. *J. Am. Ceram. Soc.*, 1980, **63**, 368–375.
30. Lange, F. F., Clarke, D. R. and Davis, B. I., Compressive creep of Si_3N_4/MgO alloys. Part 2: source of viscoelastic effect. *J. Mater. Sci.*, 1980, **15**, 611–615.
31. Burger, P., Duclos, R. and Crampon, J., Microstructure characterization in superplastically deformed silicon nitride. *J. Am. Ceram. Soc.*, in press.
32. Kijima, K. and Shirasaki, S., Nitrogen self-diffusion in silicon nitride. *J. Chem. Phys.*, 1976, **65**, 2668–2671.
33. Herring, C., Diffusional viscosity of a polycrystalline solid. *J. Appl. Phys.*, 1950, **21**, 437–445.
34. Burger, P., High temperature plasticity and deformation microstructure of silicon nitrides HIPed with Y_2O_3 and Al_2O_3 . Ph.D. thesis, University of Lille 1, Villeneuve d'Ascq, France, 1994.
35. Kessler, H., Kleebe, H.-J., Cannon, R. W. and Pompe, W., Influence of internal stresses on crystallization of intergranular phases in ceramics. *Acta Metall. Mater.*, 1992, **40**, 2233–2245.